

# 1 Evaluation of a low-cost optical particle counter (Alphasense OPC-N2) 2 for ambient air monitoring

3  
4 Leigh R. Crilley<sup>1</sup>, Marvin Shaw<sup>2</sup>, Ryan Pound<sup>2</sup>, Louisa J. Kramer<sup>1</sup>, Robin Price<sup>3</sup>, Stuart  
5 Young<sup>2</sup>, Alastair C Lewis<sup>2</sup>, Francis D. Pope<sup>1\*</sup>

6  
7 <sup>1</sup>*School of Geography, Earth and Environmental Sciences, University of Birmingham,*  
8 *Birmingham, United Kingdom, B15 2TT.*

9 <sup>2</sup>*National Centre for Atmospheric Science, Wolfson Atmospheric Chemistry Laboratories,*  
10 *University of York, York, United Kingdom, YO10 5DD.*

11 <sup>3</sup>*Birmingham Open Media (BOM), 1 Dudley Street, Birmingham, B5 4EG.*

12 \*Corresponding author – [f.pope@bham.ac.uk](mailto:f.pope@bham.ac.uk)

## 13 Abstract

14 A fast growing area of research is the development of low-cost sensors for measuring air  
15 pollutants. The affordability and size of low-cost particle sensors makes them an attractive  
16 option for use in experiments requiring a number of instruments such as high density spatial  
17 mapping. However, for these low-cost sensors to be useful for these types of studies their  
18 accuracy and precision needs to be quantified. We evaluated the Alphasense OPC-N2, a  
19 promising low-cost miniature optical particle counter, for monitoring ambient airborne  
20 particles at typical urban background sites in the UK. The precision of the OPC-N2 was  
21 assessed by co-locating 14 instruments at a site to investigate the variation in measured  
22 concentrations. Comparison to two different reference optical particle counters as well as a  
23 TEOM-FDMS enabled the accuracy of the OPC-N2 to be evaluated. Comparison of the OPC-  
24 N2 to the reference optical instruments demonstrated reasonable agreement for the measured  
25 mass concentrations of PM<sub>1</sub>, PM<sub>2.5</sub> and PM<sub>10</sub>. However, the OPC-N2 demonstrated a significant  
26 positive artefact in measured particle mass during times of high ambient RH (>85%) and a  
27 calibration factor was developed based upon κ-Kohler theory, using average bulk particle  
28 aerosol hygroscopicity. Application of this RH correction factor resulted in the OPC-N2  
29 measurements being within 33% of the TEOM-FDMS, comparable to the agreement between  
30 a reference optical particle counter and the TEOM-FDMS (20%). Inter-unit precision for the  
31 14 OPC-N2 sensors of 22±13% for PM<sub>10</sub> mass concentrations was observed. Overall, the OPC-

1 N2 was found to accurately measure ambient airborne particle mass concentration provided  
2 they are i) correctly calibrated and ii) corrected for ambient RH. The level of precision  
3 demonstrated between multiple OPC-N2 suggests that they would be suitable device for  
4 applications where the spatial variability in particle concentration was to be determined.  
5

## 6 **1.0 Introduction**

7 Airborne particles are of global concern due to their detrimental health effects, particularly in  
8 the fine fraction (PM<sub>2.5</sub>, particles with an aerodynamic diameter less than 2.5 µm) and as a  
9 result are a regulated pollutant in the EU, USA and other states. Monitoring ambient particle  
10 mass concentrations is typically performed using a small number of fixed instruments with  
11 gaps in the spatial coverage usually estimated via modeling or interpolation. This is often  
12 unsatisfactory as there can be micro-environments in urban areas that result in large spatial and  
13 temporal inhomogeneity in airborne particle concentrations, which in turn makes assessment  
14 of human exposure to airborne particles difficult (de Nazelle et al., 2017).

15 Into this gap a fast growing area is the development of low-cost sensors for measuring the  
16 concentrations of a wide range of species in the atmosphere including gases and particles  
17 (Lewis et al., 2016; Rai et al., 2017; Snyder et al., 2013). However the question remains as to  
18 whether the uncertain quality of data from these low cost sensors can be of value when  
19 attempting to determine pollutant concentrations at high spatial resolution (Kumar et al., 2015).  
20 Sensors for both gases and particles can suffer from drift and a number of interference artefacts  
21 such as relative humidity (RH), temperature and other gas phase species (Lewis et al., 2016;  
22 Mueller et al., 2017; Popoola et al., 2016). Despite these challenges, recent work has shown  
23 that low-cost gas sensors can be deployed in large scale networks provided appropriate  
24 corrections for known artefacts are applied (Borrego et al., 2016; Mead et al., 2013; Mueller et  
25 al., 2017), with clustering of multiple gas sensors into one unit shown to be an effective  
26 methodology (Lewis et al., 2016; Mueller et al., 2017; Smith et al., 2017).

27 For low-cost particle sensors, their reported performance across the literature is somewhat  
28 mixed (Borrego et al., 2016; Castellini et al., 2014; Sousan et al., 2016; Viana et al., 2015) and  
29 can depend on the type of particle sensor employed. There are a wide range of low-cost particle  
30 sensors available commercially from manufacturers including Dylos, TSI, Airsense and  
31 Alphasense. The more widely used and available low-cost particle sensors can be considered

1 as miniaturized versions of optical particle counters (OPC) and employ a light scattering  
2 technique to measure ambient particle concentrations (See e.g. (Gao et al., 2015; Sousan et al.,  
3 2016). While these miniature OPC are not meant to compete with more established  
4 instrumentation in terms of their accuracy and precision, their affordability and size makes  
5 them attractive for use in experiments requiring a number of such instruments, such as personal  
6 monitoring (See e.g. (de Nazelle et al., 2017; Steinle et al., 2015)). However to be useful in  
7 these types of studies, the precision and accuracy of these instruments needs to be evaluated.

8 Laboratory assessments of the performance of a number of low-cost miniature OPC's have  
9 shown promising results, with adequate precision observed compared to reference  
10 instrumentation (Manikonda et al., 2016). Sousan et al., (2016) evaluated the Alphasense OPC-  
11 N2 in a laboratory study using reference aerosols (Arizona road dust, NaCl and welding fumes)  
12 and found reasonable agreement for size distributions and particle mass between the OPC-N2  
13 and a GRIMM Portable Aerosol Spectrophotometer, provided appropriate and specific  
14 calibrations were applied. While these results are encouraging (Manikonda et al., 2016; Sousan  
15 et al., 2016), laboratory-based studies using reference aerosols may not be representative of  
16 their performance when measuring ambient particles, owing in part to the complex mixture and  
17 variable relative humidity and temperature encountered in the real-world. Previous field testing  
18 of low-cost particle sensors has found that the Dylos (Steinle et al., 2015), Portable University  
19 of Washington Particle (PUWP) monitors (Gao et al., 2015) performed well for ambient  
20 sampling of particle mass concentration in both an urban and rural environment when  
21 compared to reference instruments however they were assessed over a short period (4-5 days).  
22 In contrast, at a roadside location poor agreement between two different OPC sensors compared  
23 to reference instruments was observed by Borrego et al. (2016). Clearly, the results are mixed  
24 and longer-term assessment of the stability and longevity of these instruments are needed, as  
25 these are critical parameters when considering their worth for use in large-scale networks.

26 We evaluate here the Alphasense OPC-N2, a promising low-cost miniature optical particle  
27 counter (Sousan et al., 2016), for monitoring ambient airborne particles at typical urban  
28 background sites in the UK. We assessed the inter-unit precision of the OPC-N2 by co-locating  
29 14 instruments at a single site to investigate the variation in measured particle mass  
30 concentration in the  $PM_{10}$ ,  $PM_{2.5}$  and  $PM_1$  size fractions between OPC-N2. In order to  
31 determine the accuracy of the OPC-N2, we compared it to two well-established commercial

1 optical particle counters that employ a similar light scattering technique as well as a TEOM-  
2 FDMS, a regulatory standard instrument for particle mass concentration measurements.

## 3 **2.0 Method**

### 4 **2.1 Instrumentation**

#### 5 **2.1.1 Alphasense Optical particle sensor (OPC-N2)**

6 The Optical Particle Sensor (OPC) under evaluation in the current work is the OPC-N2  
7 manufactured commercially by Alphasense ([www.alphasense.com](http://www.alphasense.com)) and is described in detail  
8 in Sousan et al. (2016). The OPC-N2 can be considered as a miniaturized OPC as it measures  
9 75x60x65 mm and weighs under 105 g, and as such is significantly cheaper (approx. £200)  
10 than the comparable reference instruments (see next section). The OPC-N2 samples via small  
11 fan aspirator and measures particle number concentration over a reported size range of 0.38 to  
12 17  $\mu\text{m}$  across 16 size bins, and maximum particle count of 10,000 per second. The minimum  
13 time resolution is 10s. The measured particle number concentration is converted via on-board  
14 factory calibration to particle mass concentrations for  $\text{PM}_{10}$ ,  $\text{PM}_{2.5}$  and  $\text{PM}_{10}$  size fraction  
15 according to European Standard EN481 (OPC-N2 manual). According the OPC-N2 manual,  
16 the standard definition for  $\text{PM}_{10}$  in EN 481 extends beyond the particle size measured by the  
17 OPC-N2, and may consequently underestimate  $\text{PM}_{10}$  value by up to 10%. Further discussion  
18 on calculations for conversion from particle number to mass concentrations is given in Section  
19 2.3. All OPC-N2 in this study used firmware version 18. .

20 The OPC-N2 is designed to log data via a laptop using software supplied by Alphasense,  
21 however this may not be practical when using multiple OPC-N2 at once or for personal  
22 monitoring. Therefore, we developed a custom built system for logging the OPC-N2 during  
23 the inter-comparison, utilizing either a Raspberry Pi 3 or Arduino system. The Python code to  
24 log the outputs from OPC-N2 on a Raspberry Pi 3 is made available in the Supplementary  
25 Material. The Python code makes use of the `py-opc` python library for operating the OPC-N2  
26 written by Hagan (2017).

#### 27 **2.1.2 Reference Instruments**

28 The first reference instrument was a TSI 3330 optical particle spectrophotometer (OPS), which  
29 measures particles number concentrations between 0.3 – 10  $\mu\text{m}$  across 16 size bins, with a

1 maximum particle count of 3000 particles  $\text{cm}^{-3}$ . A GRIMM Portable Aerosol Spectrometer  
2 (PAS-1.108, forthwith referred to as the GRIMM) was also utilized, which records particle  
3 number concentrations in 15 bins from 0.3 – 20  $\mu\text{m}$ . The TSI 3330 and GRIMM were both  
4 recently calibrated and serviced. All measurements of airborne particle concentrations are  
5 inherently operationally defined and as a result the TSI 3330 and the GRIMM were chosen as  
6 reference instruments as they measure particle size in similar size bins by a similar photometric  
7 technique to the Alphasense OPC-N2.

8 For the sake of this inter-comparison, we have taken the TSI 3330 and GRIMM data as an  
9 accurate measure of particle mass concentrations. The reference instrument used for the factory  
10 calibration of the OPC-N2 by Alphasense is the TSI 3330 (Sousan et al., 2016) and hence  
11 included for comparison.

## 12 **2.2 Inter-comparison locations**

### 13 **2.2.1 Elms Rd Observatory Station**

14 The instruments were housed within the Elms Road Observatory Station (EROS) located on  
15 the University of Birmingham campus. The site is classed as urban background, with emissions  
16 from nearby road and a construction site the major sources of particles. Fourteen OPC-N2 were  
17 deployed at EROS, enabling the precision of the OPC-N2 to be assessed along with the  
18 accuracy relative to the reference instruments, the TSI 3330 and GRIMM. An intensive inter-  
19 comparison ran for just over 5 weeks, from 26<sup>th</sup> August till 3<sup>rd</sup> October 2016, during which all  
20 14 OPC-N2, TSI 3330 and GRIMM sampled ambient air. Minimal lengths (12cm) of stainless  
21 steel tubing (OPC-N2) and conductive black tubing (TSI 3330 and GRIMM) were used to  
22 sample outside air, with each OPC having its own inlet at a height of 1.5 m. The vertical inlet  
23 for the TSI 3330 necessitated a bend in the tubing, however the calculated sampling efficiency  
24 (using von der Weiden et al., 2009) was 92% for particles with a diameter of 10  $\mu\text{m}$ . Therefore,  
25 while the inlet arrangement of the TSI 3330 may have affected the inter-comparison,  
26 particularly when considering the accuracy of the OPC-N2, we were limited to what was  
27 practical. Sampling intervals for the OPC-N2, TSI 3330 and GRIMM were 10, 60 and 6  
28 seconds, respectively. In addition, RH measurements from the nearby Elms Road  
29 Meteorological station were also obtained which is located approximately 100 m away from  
30 EROS.

1 At the conclusion of the intensive inter-comparison, a subset of the OPC-N2 (5) continued to  
2 sample at EROS along with the GRIMM, to test the robustness and suitability of the OPC-N2  
3 for longer-term monitoring. The long-term monitoring concluded on 1 February 2017, meaning  
4 that these OPC-N2s sampled ambient air for up to 5 months.

### 5 **2.2.2 Tyburn Rd**

6 For regulatory purposes, an accepted method for measuring particle mass concentrations is a  
7 Tapered Element Oscillating Microbalance (TEOM) and therefore we also compared the OPC-  
8 N2 to this technique despite the difference in particle measurement approaches. An urban  
9 background air monitoring station part of the UK Automatic and Rural Urban Network  
10 (AURN) nearby EROS (Tyburn Rd) was chosen for this inter-comparison. At the Tyburn Rd  
11 AURN station, the TEOM monitor was fitted with a Filter Dynamic Measurement System  
12 (FDMS) (Grover et al., 2006), to correct for semi-volatile particle loss. A subset of OPC-N2  
13 (4) and the GRIMM PAS 1.108 that were deployed at EROS sampled at Tyburn Rd station for  
14 2 weeks during February 2017. The OPC-N2 was housed individually within waterproof boxes  
15 on the roof of the cabin near to the TEOM inlet in order to keep the inlet length the same as  
16 used at EROS. The GRIMM sampled from a nearby separate inlet.

### 17 **2.3 Data Analysis**

18 All OPC employed in this study count the number of particles and determine the size based  
19 upon particle light scattering of a laser, and to convert to particle mass concentration must  
20 apply a number of assumptions. To calculate the particle mass concentration, spherical particles  
21 of a uniform density and shape are assumed, which is not strictly true for airborne particles in  
22 an urban atmosphere but is considered a standard approximation. Therefore to ensure a fair  
23 comparison between the different OPC, the same calculations and assumptions must be applied  
24 to all three OPC measurements. The TSI 3330 data was processed using the TSI AIM software  
25 to convert the particle count concentration to particle mass measurements. The particle counts  
26 from the GRIMM data was converted to particle mass (via particle volume) using the same  
27 calculations, as outlined in the TSI AIM software manual according to Equations 1 to 3:  
28

$$29 \quad D_{pv} = LB \left[ \frac{1}{4} \left( 1 + \left( \frac{UB}{LB} \right)^2 \right) \left( 1 + \left( \frac{UB}{LB} \right) \right) \right]^{\frac{1}{3}} \quad (1)$$

1 
$$v = \frac{\pi D_{pv}^3 n}{6} \tag{2}$$

2 
$$m = \rho v \tag{3}$$

3 where  $D_{pv}$  is the volume weighted diameter, LB the channel lower boundary, UB the channel  
4 upper boundary,  $v$  is the particle volume for a channel,  $n$  is number weighted concentration per  
5 channel,  $m$  is the particle mass per channel and  $\rho$  is the particle density.

6 The OPC-N2 converts, on board via a factory determined calibration, particle counts to particle  
7 mass concentration in  $PM_1$ ,  $PM_{2.5}$  and  $PM_{10}$  mass concentrations. There is no further  
8 information provided by Alphasense on how this calculation is performed apart from the  
9 applied particle density across all size bins was  $1.65 \text{ g cm}^{-3}$ . Therefore, we assumed calculations  
10 are similar to Eqns 1 and 2 as applied to the TSI and GRIMM data and used the same particle  
11 density (1.65) across all size bins to calculate particle mass for all OPC.

12 All instrument time series were corrected for drift against a reference time. As the sampling  
13 intervals varied slightly between the different OPC, a 5 min average of particle concentrations  
14 was used for inter-comparison between instruments.

## 15 **3.0 Results and Discussion**

### 16 **3.1 EROS inter-comparison**

#### 17 **3.1.1 Comparison of reference optical light scattering instruments**

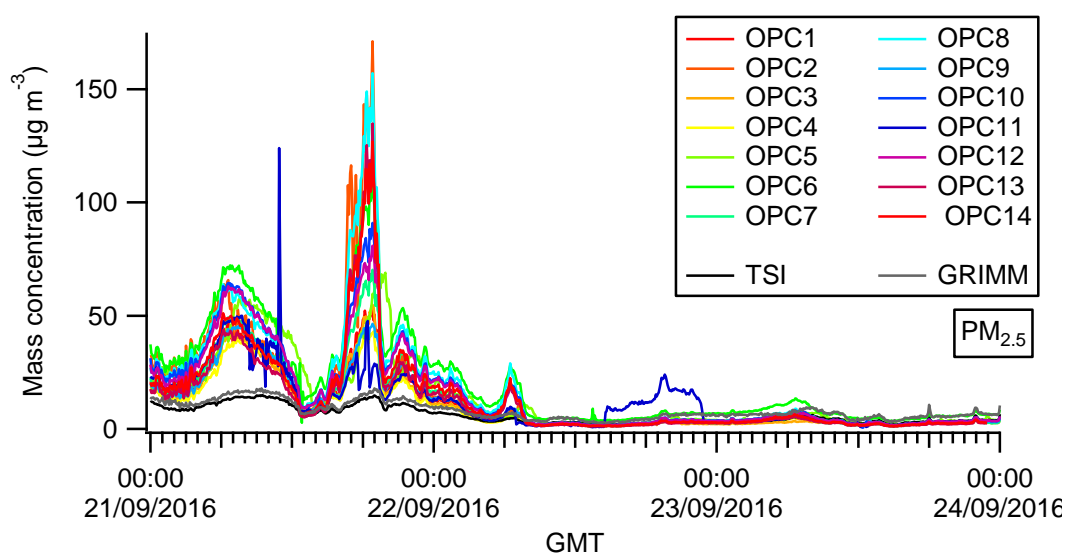
18 The two light scattering optical particle counters used as reference instruments in this study  
19 were found to be well correlated ( $r^2 > 0.9$ ), with the GRIMM recording between 20-30% higher  
20 concentrations for all three particle mass fractions (Fig S1, Supporting Information). The  
21 GRIMM is known to overestimate number concentration (Sousan et al., 2016 and references  
22 therein) and this difference may reflect differing efficiencies in particle detection between the  
23 two instruments.

#### 24 **3.1.2 Performance of the OPC-N2**

25 The performance of the custom built logging systems varied between 44-94% successful data  
26 capture, with the Arduino and Raspberry Pi systems giving 44-65% and >92%, respectively.  
27 The Raspberry Pi data logger system was used for the long-term measurements and for the

1 inter-comparison with the AURN site due to its better performance. The data losses were due  
 2 to hardware issues and not related to performance of the OPC-N2. Due to the missing data,  
 3 only a subset of measured PM<sub>2.5</sub> concentrations when all 14 OPC-N2 were logging are shown  
 4 in Fig 1, along with measured concentrations by the reference instruments. From Fig 1, while  
 5 there are times when there appears to be excellent agreement between the OPC-N2 and the  
 6 reference instruments, there are times when the OPC-N2 record a significant positive artefact,  
 7 and during these times the spread in measured concentrations increases. For example, on the  
 8 morning of the 18th September, the range of measured concentrations by the individual OPC-  
 9 N2 was from approximately 30-150  $\mu\text{g m}^{-3}$ , whereas the reference instruments reported  $\sim 10 \mu\text{g m}^{-3}$ .  
 10 The cause of the positive artefact is investigated in later sections, but it points to the  
 11 individual OPC-N2 responding differently to this artefact. Similar trends were also observed  
 12 for PM<sub>1</sub> and PM<sub>10</sub>, see Figure S2 in the Supporting Information.

13  
 14



15  
 16 Figure 1: Time series of PM<sub>2.5</sub> concentrations measured by all OPC-N2 and the reference  
 17 instruments, TSI 3330 and GRIMM for selected period with high OPC-N2 data coverage.

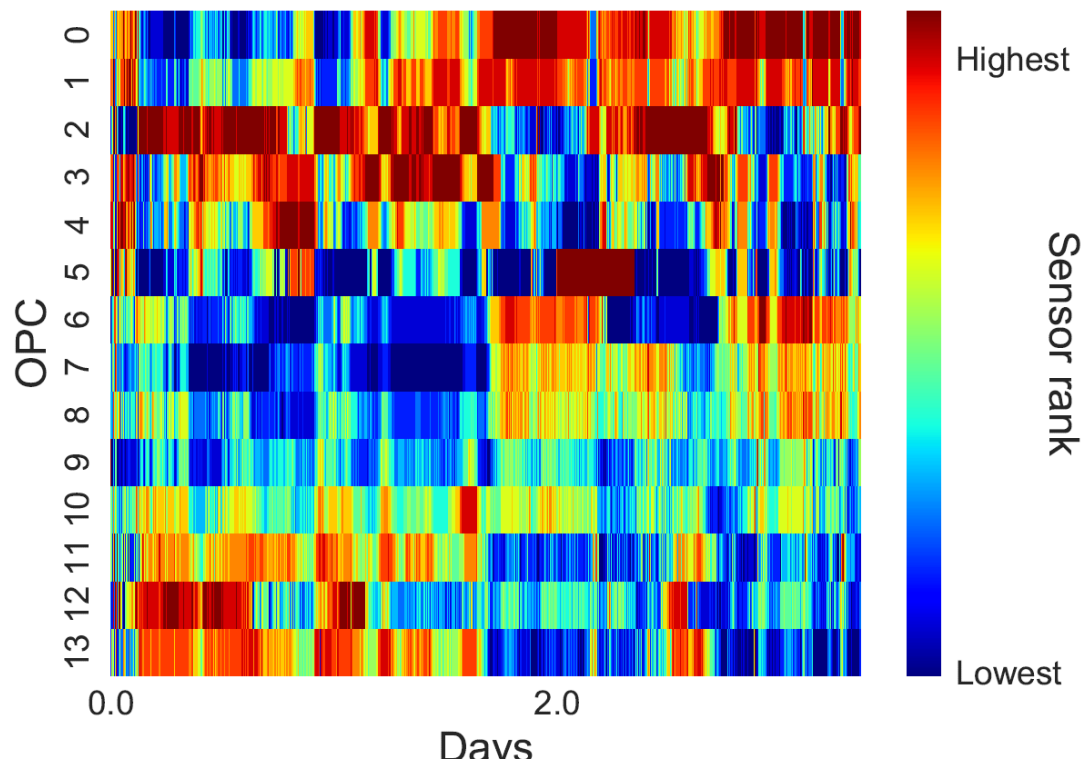
18  
 19 As there is a considerable spread in response for the OPC-N2 relative to the reference  
 20 instruments, we then quantified whether it was always the same OPC-N2 reading low and high.  
 21 Due to the aforementioned data capture issues, this analysis was only applied to days when all  
 22 14 OPC-N2 were running, 21<sup>st</sup>-24<sup>th</sup> September (Fig 1). The results are shown as a rank order  
 23 plot, where the OPC-N2 observations are ordered from the highest reported value to the lowest  
 24 over this period, normalised to the median concentration at the start of the analysis (t=0), shown



1 for PM<sub>2.5</sub> mass concentration in Figure 2. The ranking of the OPC-N2's showed some  
2 variability over time within periods of 1-6 hours, which was particularly noticeable during  
3 periods when the OPC-N2 signals underwent large changes in concentrations. This  
4 demonstrates that the highest and lowest reporting OPC was not consistently reporting the  
5 highest and lowest the lowest PM<sub>2.5</sub> concentrations, respectively over the whole 3 day period.  
6 The same trend was also observed for PM<sub>1</sub> and PM<sub>10</sub> mass concentrations, as shown in Figure  
7 S3 (Supporting Information).

8  
9 For the 3 day time period (21<sup>st</sup>-24<sup>th</sup> of September) we applied the rank order analysis, two  
10 subsets of concentrations measured by the OPC-N2 were evident in the time series (Fig 1); one  
11 a period of highly variable mass concentrations (0:00 21/9/16 to 12:00 22/9/16) of September)  
12 followed by more stable mass concentrations (12:00 22/9/16 onward). This was reflected in the  
13 corresponding rank order plots where relatively consistent OPC rank orders were observed  
14 throughout the variable and comparatively stable PM concentrations periods. However, there  
15 is a noticeable transition between the two periods in the rank order plot, observed at  
16 approximately 12:00 on the 22<sup>nd</sup>). This transition in rank orders would reflect the difference in  
17 OPC PM sensitivities, random noise and offset values between each OPC. Over the 3 day  
18 period the OPCs appeared to hold their response characteristics and hence rank orders well,  
19 suggesting that over this timescale quantitative concentrations could be directly compared. Due  
20 to the changing response and the incomplete data coverage, for the rest of the analysis in this  
21 paper, when comparing to the reference instruments the median and inter-quartiles  
22 concentrations of all 14 OPC-N2 were used.

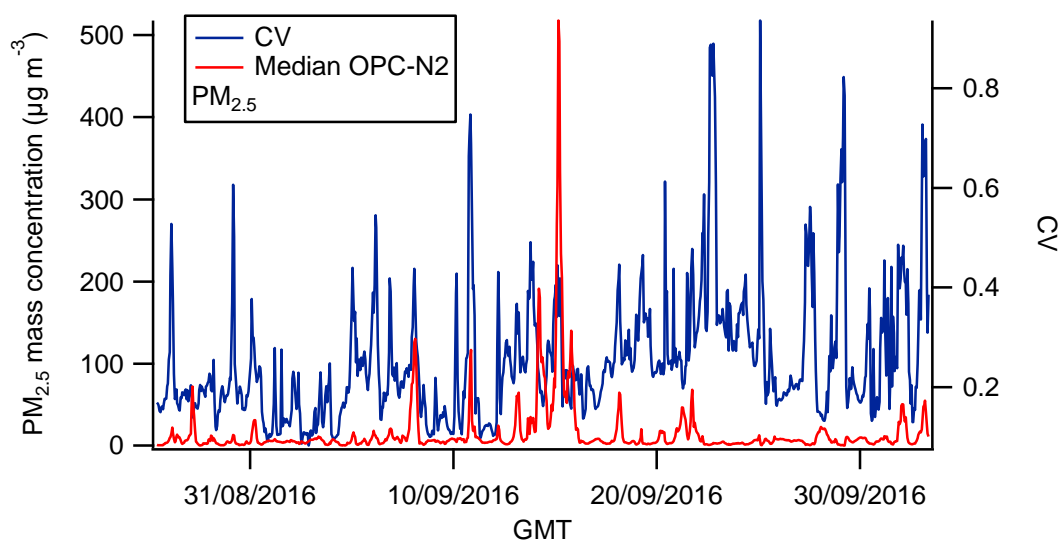
23



1  
2  
3  
4  
5  
6  
7  
8  
9  
10  
11  
12  
13  
14  
15  
16  
17  
18  
19  
20

Figure 2: Sensor ranking analysis for measured  $PM_{2.5}$  mass concentrations for the 14 OPC-N2 over a 3 day period (21st-24th of September) with high OPC-N2 data coverage.

One measure of the precision of a group of instruments is the coefficient of variance (CV) and this was calculated for the measured ambient mass concentrations of all 14 OPC-N2 to assess the variability between 14 instruments. The average CV was  $0.32 \pm 0.16$ ,  $0.25 \pm 0.14$  and  $0.22 \pm 0.13$  for  $PM_1$ ,  $PM_{2.5}$  and  $PM_{10}$  mass concentrations, respectively. This is higher than the value of 0.1 considered acceptable for duplicate instruments by the US EPA (see Sousan et al., 2016 and references therein) but perhaps not unreasonable for low-cost sensors. This may in part be due the OPC-N2 all sampling from separate but identical inlets but suggests the precision of the OPC-N2 would need to be considered when comparing multiple units. To analyse whether the CV for the OPC-N2 varied over the month, the median concentration was plotted along with the CV (shown for  $PM_{2.5}$  in Fig 3). Throughout the measurement period, the CV was fairly consistent (mean of  $0.22 \pm 0.13$ ), with spikes in CV values evident during periods of high  $PM_{2.5}$  concentrations, in agreement with trends observed in Fig 1. We observed a similar trend of consistent CV values for both  $PM_1$  and  $PM_{10}$  concentrations suggesting reasonably stable agreement between all OPC-N2 over a 5 week period.



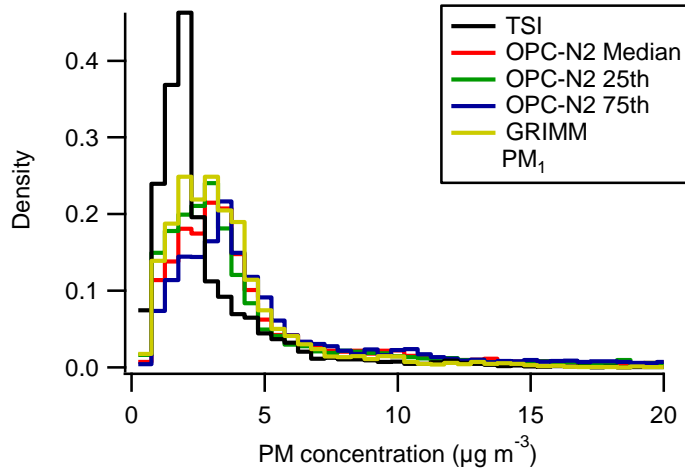
1  
 2 Figure 3: Time series of the hourly average median OPC and CV during the September  
 3 intensive inter-comparison at EROS for PM<sub>2.5</sub> mass concentration.

#### 4 **3.2 Comparison of Alpha sense OPC to reference instruments**

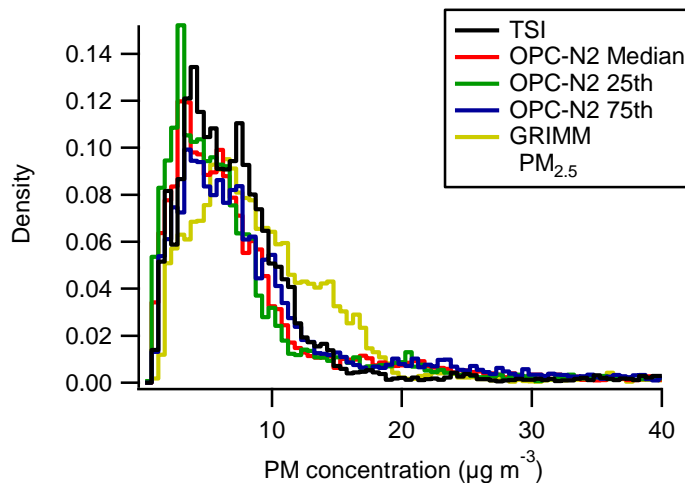
##### 5 **3.2.1 Particle mass concentration measurement at EROS**

6  
 7 The median and inter-quartiles of the measured PM concentrations from the 14 OPC-N2 were  
 8 used to compare the measured particle mass concentrations to the reference instruments (Figure  
 9 4). From Fig 4, the notably similar distributions across all three particle size fractions for the  
 10 first and third quartiles indicate good agreement between the 14 OPC-N2, further highlighting  
 11 the reasonable degree of precision between the OPC-N2 as shown in the previous section. At  
 12 typical ambient PM<sub>2.5</sub> and PM<sub>10</sub> mass concentrations for the UK, similar distributions were  
 13 observed for the OPC-N2 and reference instruments (Fig 1), suggesting reasonable agreement  
 14 between the devices. In contrast, different distributions were observed for the PM<sub>1</sub> fraction,  
 15 with the OPC-N2 and GRIMM in agreement but appearing to over-estimating the PM<sub>1</sub> mass  
 16 concentrations with respect to the TSI 3330. While the OPC-N2 has a higher particle size cut-  
 17 off (0.38 µm) compared to the TSI (0.3µm) and may explain the observed difference in  
 18 frequency distribution for PM<sub>1</sub> (Fig 1). While the TSI and GRIMM have the same particle size  
 19 cut-off (0.3 µm), these instruments have been shown to disagree (Fig S1) possibly due to  
 20 different particle collection efficiencies.

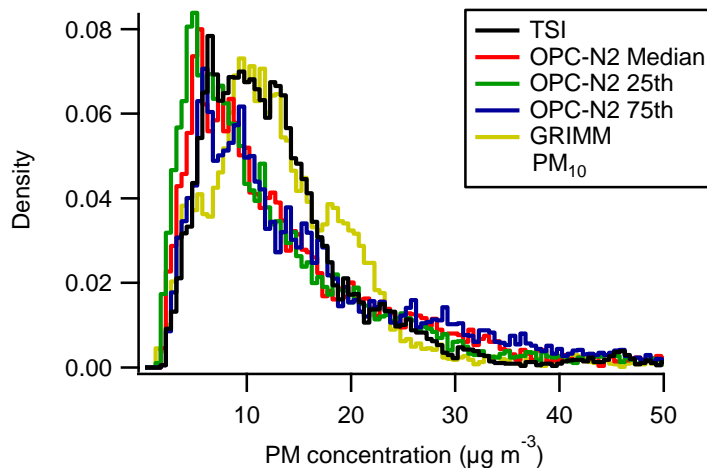
21



1



2



3

4 Figure 4: Histogram of measured PM<sub>1</sub>, PM<sub>2.5</sub> and PM<sub>10</sub> mass concentrations by the TSI 3330,  
 5 GRIMM and median and inter-quartile values for the 14 OPC-N2. Note the different x and y  
 6 axis scales.

7 When the median and inter-quartile OPC-N2 concentrations were plotted against the TSI and  
 8 GRIMM concentrations, the slope was greater than unity for all three size fractions (Table 1)

1 indicating that the OPC-N2 were over-estimating the ambient particle mass concentrations  
 2 (approx. 2 to 5 times, Table 1). Overall, the OPC-N2 and GRIMM were in better agreement  
 3 compared to the TSI for all size fractions (Table 1). The GRIMM was found to record PM  
 4 concentrations 20-30% higher compared to the TSI (Figure S1), and this could in part account  
 5 for the observed lower slopes between the GRIMM and the OPC-N2.

6 Table 1: Slopes of measured PM mass concentrations of the reference instruments against the  
 7 median and inter-quartiles for OPC-N2. The intercepts were not constrained to zero.  
 8 Correlation co-efficient,  $r^2$  is given in parenthesis.

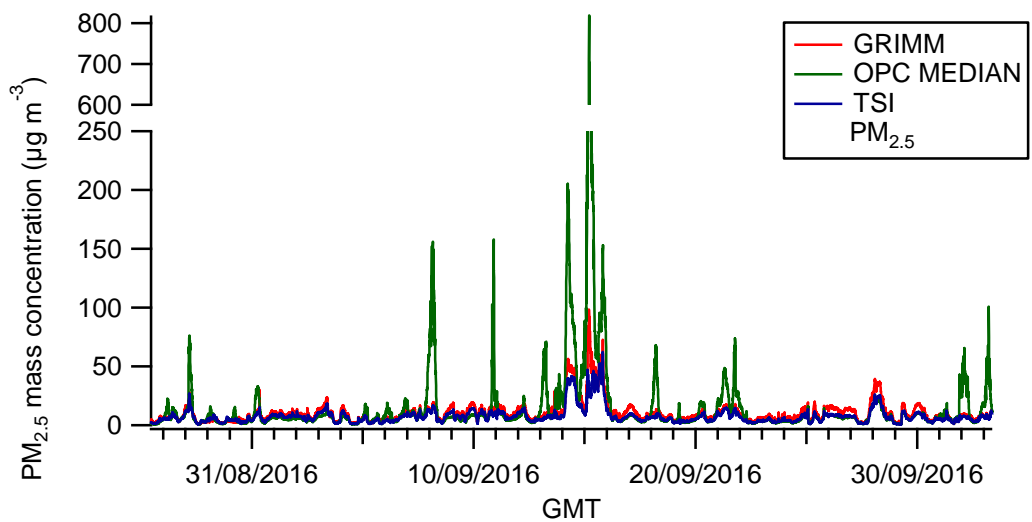
	<b>PM<sub>1</sub></b>		<b>PM<sub>2.5</sub></b>		<b>PM<sub>10</sub></b>	
	<i>OPC-N2</i>	<i>TSI</i>	<i>GRIMM</i>	<i>TSI</i>	<i>GRIMM</i>	<i>TSI</i>
<b>25<sup>th</sup></b>	2.93+0.01 (0.9)	2.34+0.1 (0.92)	3.16+0.03 (0.66)	2.62+0.02 (0.77)	2.05+0.02 (0.64)	1.85+0.02 (0.6)
<b>Median</b>	3.19+0.02 (0.86)	2.63+0.01 (0.91)	3.53+0.04 (0.63)	3.02+0.03 (0.76)	2.29+0.03 (0.57)	2.06+0.02 (0.67)
<b>75<sup>th</sup></b>	3.90+0.02 (0.87)	3.24+0.02 (0.89)	4.77+0.06 (0.59)	4.21+0.04 (0.71)	2.73+0.04 (0.53)	2.47+0.35 (0.57)

9  
 10 The time series of the median OPC-N2 PM<sub>2.5</sub> concentrations along with the two reference  
 11 instruments are shown in Figure 5, and for a large portion of the inter-comparison all  
 12 instruments appear to be in agreement. However, there were a number of times when the OPC-  
 13 N2 readings were up to an order of magnitude higher relative to the reference (e.g. 15<sup>th</sup>  
 14 September), pointing to a significant instrument artefact. On the 15<sup>th</sup> September, the GRIMM  
 15 and TSI also move out of agreement and may point to the same artefact affecting the GRIMM.  
 16 Similar trends were also observed for the PM<sub>1</sub> and PM<sub>10</sub> mass fractions (Fig S4, Supporting  
 17 Information) with the OPC-N2 over-estimating the PM<sub>10</sub> concentration by several orders of  
 18 magnitude on 15<sup>th</sup> September (peak mass concentrations in the order of 15,000  $\mu\text{g m}^{-3}$ ). Note  
 19 that as EROS is an urban background site, it was unlikely to be affected by plumes from sources  
 20 such as vehicles and as a result these high concentrations spikes may not be real.

21  
 22 The factors contributing to this apparent artefact shown by the OPC-N2 were investigated. In  
 23 Fig 6, the agreement between the OPC-N2 and the TSI instrument appears to vary as a function  
 24 of ambient RH, with better agreement observed between the two instruments during periods of  
 25 relatively low ambient RH. However, during times when the RH was high (>90%), the OPC-

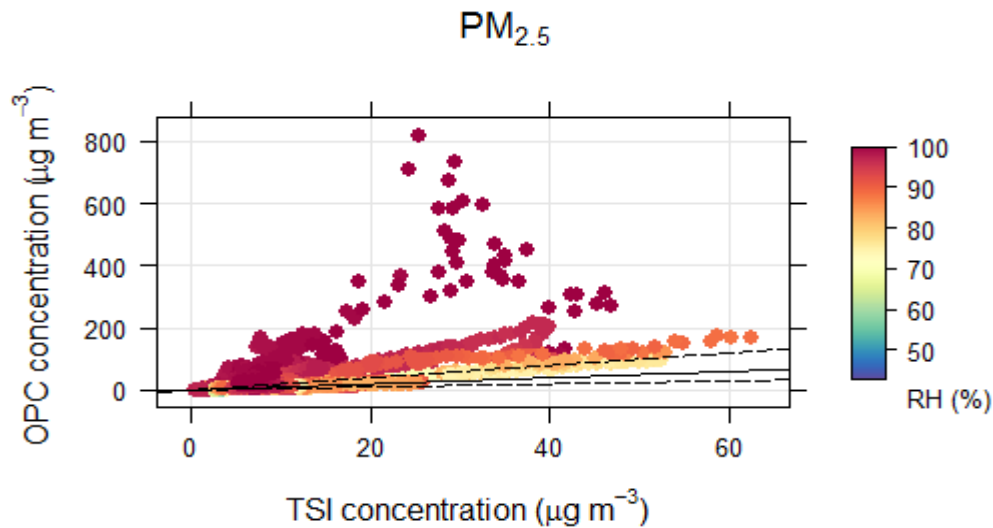
1 N2 recorded concentrations markedly higher than that measured by the TSI 3330 (Fig 6).  
2 Similar trends were also observed for PM<sub>1</sub> and PM<sub>10</sub> mass concentrations (Figure S5,  
3 Supporting Information). Thus, it points to ambient RH as a significant contributing factor  
4 affecting the particle mass concentrations measured by the OPC-N2, and this is tested further  
5 in later sections. There are distinct differences in design in OPC-N2 compared to the reference  
6 instruments (GRIMM and TSI 3330) as both the TSI 3330 and GRIMM utilise a sheath flow  
7 unlike the OPC-N2. The sheath flow in both devices will be warmed to temperatures higher  
8 than the ambient air due to proximity to the instrument pumps and electronics. This would  
9 mean that they measure at a lower RH than ambient and could explain why no RH dependence  
10 was observed on measured particle concentrations by the GRIMM and TSI 3330.

11  
12  
13



14  
15  
16  
17

Figure 5: Time series of the measured PM<sub>2.5</sub> mass concentrations by the TSI, GRIMM and median concentration measured by the 14 OPC-N2 at EROS.



1  
 2 Figure 6: Measured concentrations by the TSI 3330 compared to the median concentration  
 3 measured by the 14 OPC-N2, coloured by the ambient relative humidity. Also shown are the  
 4 1:1 (solid) and 0.5:1 and 2:1 (dashed) lines.

5

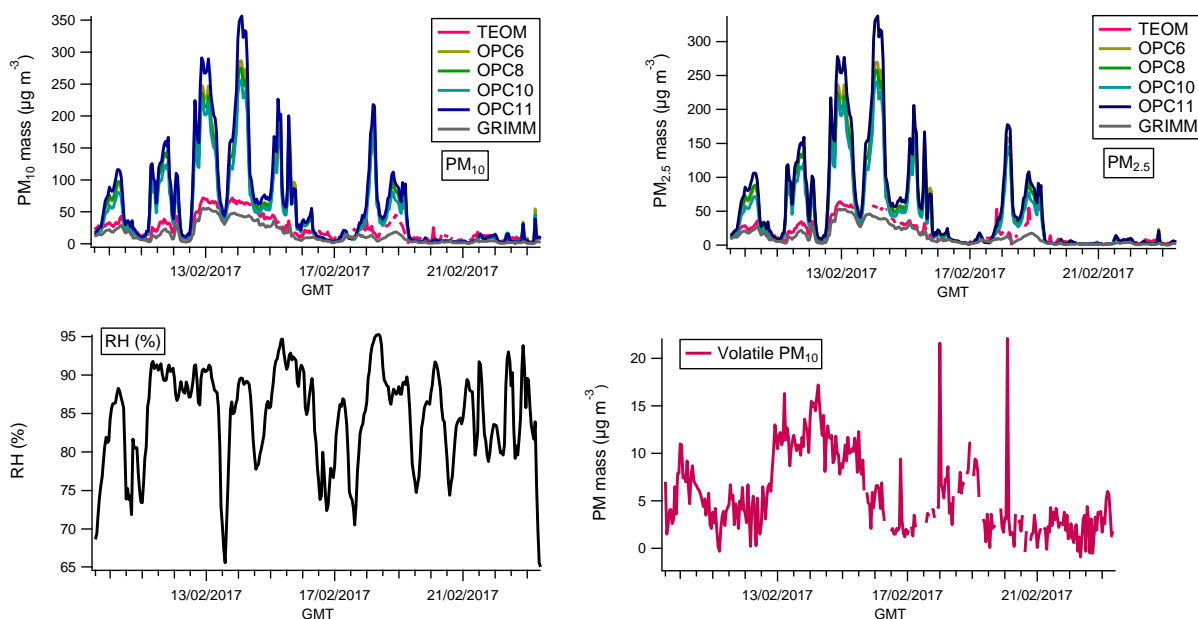
### 6 **3.2.3 Comparison to TEOM-FDMS at AURN monitoring station**

7

8 We deployed a subset of the OPC-N2 devices (4) and the GRIMM at an urban background  
 9 AURN station, to enable comparison of the measured ambient particle mass concentrations to  
 10 a TEOM-FDMS. The time series of the measured concentrations of  $PM_{10}$  and  $PM_{2.5}$  for all  
 11 instruments is shown in Fig 7. The two reference instruments were found to be well correlated  
 12 ( $r^2 > 0.91$ , Figure S6, Supporting Information) but with the GRIMM reading was about 20%  
 13 lower than the TEOM, in agreement with previous work (Grover et al., 2006). From Fig 6,  
 14 periods of agreement between the four OPC-N2 and the reference instruments (GRIMM and  
 15 TEOM) were apparent, along with times when the four OPC-N2 measured concentrations that  
 16 were notably higher than the reference instruments. Overall, when compared to the TEOM, the  
 17 OPC-N2 measurements were 2.5-3.9 times higher for both the  $PM_{10}$  and  $PM_{2.5}$ , with  
 18 considerable scatter observed (Table 2).

19

20



1

2

3

4 Figure 7: Time series for hourly measured PM mass concentrations by the TEOM, four OPC-  
 5 N2 and GRIMM at Tyburn Rd urban background AURN station. The volatile particle mass  
 6 concentration as measured by the TEOM-FDMS and relative humidity measured at Tyburn Rd  
 7 also shown.”

8

9 Closer inspection of Fig 7 indicated that the times when the four OPC-N2 over-estimated the  
 10 particle mass concentrations were during times of high RH (e.g. 12-14<sup>th</sup> Feb), as observed in  
 11 the previous section. However, there were periods of high RH when the four OPC-N2 and  
 12 TEOM were in better agreement (e.g. 20<sup>th</sup> Feb onwards), indicating that the large positive  
 13 artefact observed in the OPC-N2 was not just related to RH. Rather, it appears that positive  
 14 artefact was observed during times when the volatile fraction measured by the TEOM was  
 15 relatively high, as well as higher RH, as was observed on 12-14<sup>th</sup> Feb (Fig 7). Thus, it suggests  
 16 that the ambient aerosol composition also contributed to the significant positive artefact in the  
 17 OPC-N2. A recent laboratory study found that the particle mass concentrations measured by  
 18 OPC-N2 for all three size fractions were highly linear with respect to gravimetrically corrected  
 19 reference instruments but that the slope was dependent on the aerosol type (Sousan et al., 2016).  
 20 Sousan et al. (2016) observed in the PM<sub>10</sub> fraction slopes greater than unity for Arizona road  
 21 dust but less than unity for salt and therefore suggest that changes in aerosol composition may  
 22 also account for the differences observed between the reference instruments and OPC-N2 (Figs  
 23 7). This result highlights a limitation when comparing optical methods to gravimetric - as



1 differences may be due to changes in particle mass, size distribution or composition: as all can  
 2 affect the ability of a particle to scatter light (Holstius et al., 2014).

3  
 4 From Fig 6, the times when there was a large positive artefact in the OPC-N2 occurred when  
 5 the RH was above 85%. If we exclude these times when the RH was over this threshold, better  
 6 agreement between the four OPC-N2 and the TEOM was observed, with slopes between 1.1-  
 7 1.7 for both size fractions (Table 2). One of the OPC-N2 recorded notably higher mass  
 8 concentrations compared to the reference instruments (OPC11), compared to the other three  
 9 OPC-N2 (Table 2), and this highlights the need to calibrate each OPC individually before use  
 10 in field measurements.

11  
 12 Table 2: Slopes of measured PM mass concentrations of the reference instruments (TEOM and  
 13 GRIMM) against the OPC-N2. The correlation co-efficient,  $r^2$  is given in parenthesis. The  
 14 intercepts were not constrained to zero.

		PM <sub>10</sub>				PM <sub>2.5</sub>			
		OPC6	OPC8	OPC10	OPC11	OPC6	OPC8	OPC10	OPC11
<b>ALL</b>	TEOM	2.6 (0.64)	2.8 (0.68)	2.5 (0.64)	3.5 (0.67)	3.3 (0.7)	3.1 (0.74)	2.9 (0.7)	3.9 (0.72)
	GRIMM	3.7 (0.66)	3.6 (0.69)	3.2 (0.66)	4.4 (0.68)	3.8 (0.71)	3.7 (0.74)	3.4 (0.71)	4.6 (0.72)
	TEOM	1.4 (0.82)	1.4 (0.83)	1.2 (0.83)	1.7 (0.83)	1.3 (0.79)	1.4 (0.8)	1.1 (0.79)	1.6 (0.79)
	GRIMM	1.8 (0.83)	1.9 (0.84)	1.6 (0.84)	2.2 (0.84)	2.0 (0.89)	2.1 (0.89)	1.7 (0.9)	2.4 (0.88)

### 17 3.3 Development of correction factor for ambient RH

18 Clearly there were times when there was a significant instrument artefact for the OPC-N2 (Figs  
 19 4 and S4) and the highest over-estimations occurred at high RH at both EROS and Tyburn Rd  
 20 (e.g. Fig 5 and 6). Whilst the accuracy of the instrument was significantly worse at high  
 21 RH the precision remains the same within error. The CV analysis conducted in section  
 22 3.1.2 is repeated for the same dataset but put into low (RH<85%) and high RH (RH>85%)  
 23 subsets. For high RH conditions the CV for PM<sub>1</sub>, PM<sub>2.5</sub> and PM<sub>10</sub>, was 0.34±0.30, 0.27±0.14

1 and  $0.23 \pm 0.21$ , respectively. For low RH conditions the CV for  $PM_{10}$ ,  $PM_{2.5}$  and  $PM_{10}$ , was  
2  $0.30 \pm 0.25$ ,  $0.23 \pm 0.14$  and  $0.20 \pm 0.18$ , respectively.

3

4 The size of hygroscopic particles is known to be dependent on RH, as the particle refractive  
5 index and size are both a function of RH. Inorganic aerosols (e.g. sodium chloride, nitrate and  
6 sulphate), make up a large portion of the  $PM_{10}$  observed at EROS (Yin et al., 2010), and are  
7 known to demonstrate an exponential increase in hygroscopic growth at high RH (e.g. (Hu et  
8 al., 2010; Pope et al., 2010).

9

10 The ratio of measured mass concentrations by the OPC-N2 relative to the reference instruments  
11 was plotted as a function of RH, and appeared to show an exponential increase above ~85%  
12 RH, similar to hygroscopic particle growth curves (Pöschl, 2005). As a result, we applied  $\kappa$ -  
13 Kohler theory (Petters and Kreidenweis, 2007), which describes the relationship between  
14 particle hygroscopicity and volume by a single hygroscopicity parameter,  $\kappa$ . The  $\kappa$ -Kohler  
15 theory can be adapted to relate particle mass to hygroscopicity at a given RH by equation 5  
16 (Pope, 2010):

17

$$18 \quad a_w = \frac{(m/m_o - 1)}{(m/m_o - 1) + (\frac{\rho_w}{\rho_p} \kappa)} \quad (5)$$

19

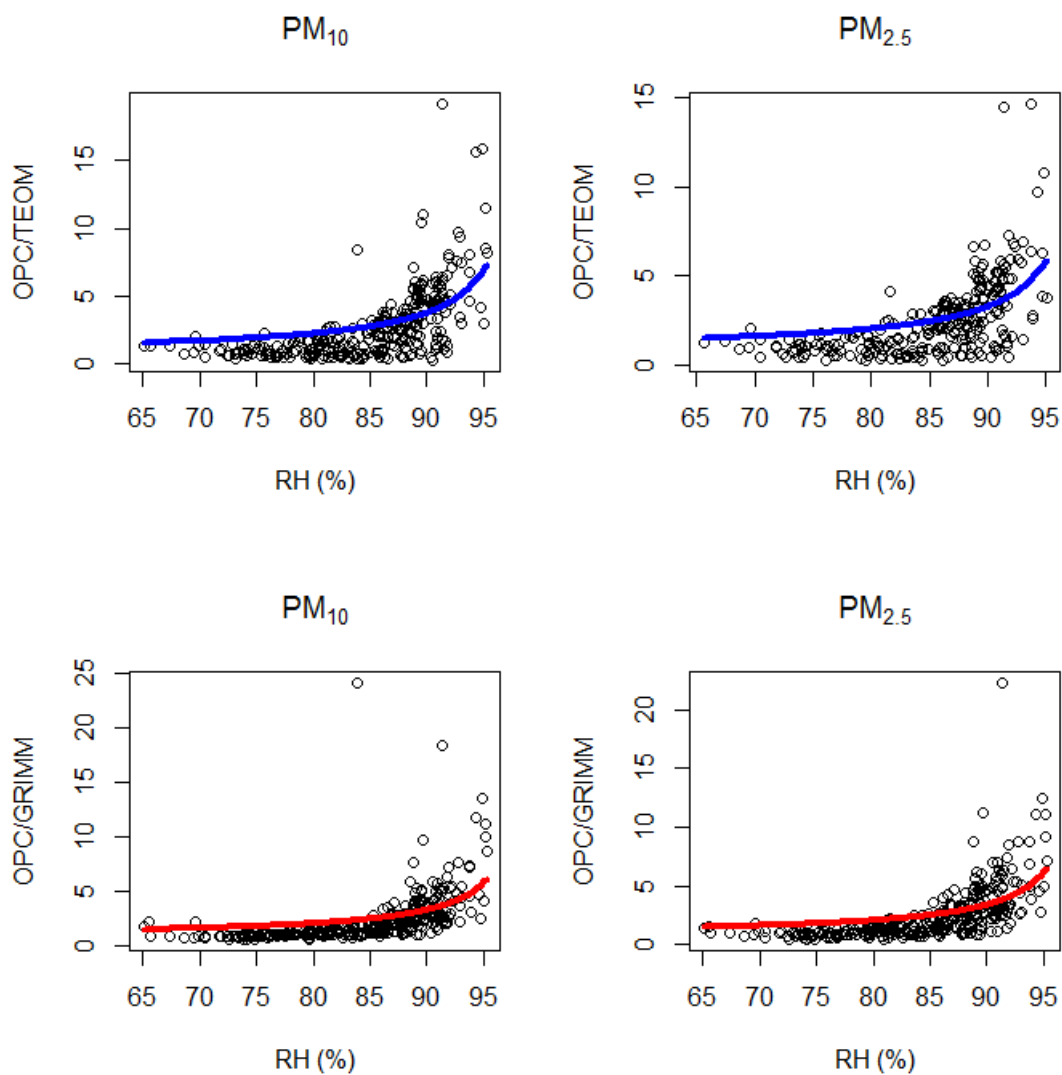
20 Where  $a_w$  is the water activity ( $a_w = \text{ambient RH}/100$ ),  $m$  and  $m_o$  are the wet and dry (RH = 0%)  
21 aerosol mass, respectively. The density of the dry particles and water is given by  $\rho_w$  and  $\rho_p$ ,  
22 respectively. The density of water is  $1 \text{ g cm}^{-3}$ , and the bulk dry particle density is assumed to  
23 be  $1.65 \text{ g cm}^{-3}$ . The value for  $\kappa$  can be found by a non-linear curve fitting of a humidogram  
24 ( $m/m_o$  vs  $a_w$ ), and was calculated using the TEOM measurements at Tyburn Rd in the first  
25 instance as the TEOM system employs a Nafion dryer and so measures dry particle mass  
26 (Grover et al., 2006). To account for the differences in mass concentration measured by the  
27 TEOM and OPC-N2 at RH less than 85%, the scaling factors shown in Table 2 are used  
28 calibrate the dry mass of the OPC-N2 to that observed in the TEOM, both in the  $PM_{2.5}$  and  
29  $PM_{10}$  fractions.

30

31 Figure 8 shows the humidogram plots, for both the  $PM_{2.5}$  and  $PM_{10}$  fractions, obtained by  
32 plotting the ratio of OPC-N2 to the reference instrument (TEOM and GRIMM) outputs versus  
33 RH. When using the TEOM for  $m_o$ , similar  $\kappa$  constants were calculated for all OPC-N2,

1 ranging from 0.38-0.41 and 0.48-0.51 for  $PM_{2.5}$  and  $PM_{10}$ , respectively, which is within the  
 2 expected range for Europe ( $0.36 \pm 0.16$ , (Pringle et al., 2010)). Similar  $\kappa$  values were observed  
 3 when using the GRIMM mass concentrations as the dry particle mass ( $m_0$ ), ranging from 0.41-  
 4 0.44 and 0.38-0.41 for  $PM_{2.5}$  and  $PM_{10}$ , respectively.

5  
6



8  
 9 Figure 8: Measured and fitted humidograms ( $m/m_0$  vs RH) recorded at the Tyburn Road AURN  
 10 site for  $PM_{10}$  and  $PM_{2.5}$  size fractions and reference instruments (TEOM and GRIMM). The  
 11 dry mass ( $m_0$ ) is given by the TEOM or GRIMM and the humidified mass is given by the  
 12 OPC-N2. Measured data is given by the black circles, the fitted data is given by the blue  
 13 (TEOM-FDMS) and red (GRIMM) line.

14

1 We then applied this fitting constant to model the expected OPC/Reference instrument ratio  
2 for a given RH as a result of particle hygroscopic growth, by re-arranging Equation 5:

$$3 \frac{m}{m_o} = 1 + \frac{\frac{\rho_w \kappa}{\rho_p}}{-1 + \frac{1}{a_w}} \quad (6)$$

5  
6 Where the  $m/m_o$  is the ratio of the OPC-N2 to the reference instruments. Using Equation 6, the  
7 mass concentrations measured by the OPC-N2 were corrected and significantly better  
8 agreement between the corrected OPC-N2 and reference instruments was observed for  
9 measurements across the whole range of ambient RH (Tables 2 and 3). Overall, the corrected  
10 OPC-N2 mass concentrations using Eqn 6 were notably better, within 33% and 52% of the  
11 TEOM and GRIMM, respectively. (Table 3) compared to 250-400% without the correction  
12 factor (Table 2). The time series for the corrected data is shown in Figures S7 and S8  
13 (Supporting Information) and there are periods where there is good agreement between TEOM  
14 and the corrected OPC-N2.

15 There were also times when the OPC-N2 were clearly over-corrected (e.g. from 20<sup>th</sup> February  
16 onwards), generally when the ambient RH was low (Fig 6). This suggests that when the RH  
17 was below a threshold, Eqn 6 overcorrects the data and this can be observed in the  
18 humidograms shown in Figure 8. Typically, at RH <85% the hygroscopic growth of real  
19 atmospheric aerosols is small and it may be more appropriate to apply a linear regression  
20 correction factor for data recorded under these RH conditions. Therefore we applied a binary  
21 two model approach to correct the OPC-N2 mass concentrations, where a linear  
22 correction (using the TEOM as reference concentration) for when RH <85%, and above  
23 this threshold in RH Eqn 6 was used. As can be seen Figure S9 (Supporting Information),  
24 there was little change in the slope or  $r^2$  value with the two model correction compared  
25 to the using correction with Eqn 6 for all RH. What was noticeable was that the intercept  
26 for the two model approach moved closer to zero, suggesting that at the lower mass  
27 concentrations the correction was improved. Similar trends were also observed for PM<sub>10</sub>.  
28 Also during the period from the 20<sup>th</sup> February, the volatile particle fraction was also lower (Fig  
29 6) and this indicates a significantly different aerosol composition. Since  $\kappa$  is composition  
30 dependent, a single global fit to  $\kappa$  will result in poor fitting when the true  $\kappa$  is significantly  
31 different to the average  $\kappa$ . The preceding discussion suggests that further refinement to the

1 correction factors applied to the OPC-N2 is possible, depending on the ambient RH and better  
 2 knowledge of aerosol composition. RH measurement is relatively trivial and can be achieved  
 3 with small sensors but aerosol composition determination still requires significant analytical  
 4 equipment and expertise.

5

6 Table 3: Summary of the comparison between the corrected OPC-N2 (via Eqn 6) against the  
 7 reference instruments. Intercepts were not constrained to zero.

OPC-N2	TEOM		GRIMM	
	$PM_{2.5}$	$PM_{10}$	$PM_{2.5}$	$PM_{10}$
<b>OPC6</b>	1.08±0.03	0.87±0.02	1.26±0.03	1.27±0.03
<b>OPC8</b>	1.11±0.03	0.89±0.02	1.29±0.03	1.23±0.03
<b>OPC10</b>	0.98±0.03	0.80±0.02	1.16±0.03	1.17±0.03
<b>OPC11</b>	1.33±0.04	1.06±0.03	1.53±0.04	1.51±0.04

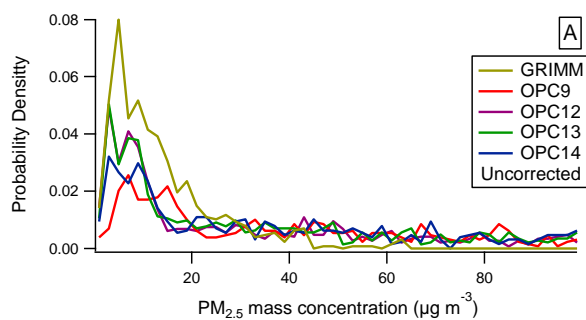
8

### 9 3.3.1 Longer-term monitoring with OPC-N2 at EROS

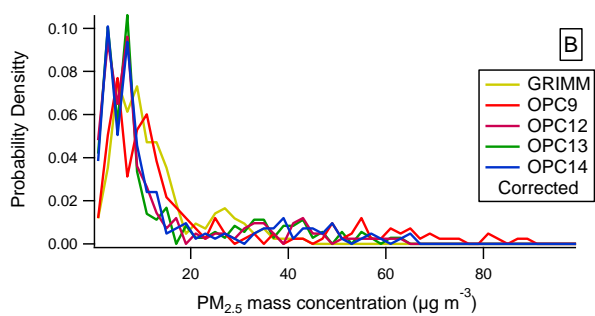
10

11

12



13



14

15 Figure 9: Histogram of measured  $PM_{2.5}$  concentrations by the GRIMM PAS 1.108 and the 4  
 16 OPC-N2s for January. The uncorrected OPC-N2 concentrations are shown in the left plot (A),  
 17 while the right plot (B) shows the RH corrected OPC-N2 concentrations.

1  
2 After the conclusion of the intensive measurements at EROS (Section 3.1), five of the OPC-  
3 N2 continued monitoring for a further 4 months to examine if there was any evidence of  
4 instrument drift over time, along with the GRIMM as reference. One of the OPC-N2 failed in  
5 December, and so was excluded from this analysis. The remaining four OPC-N2 were  
6 compared to GRIMM and in January after running for 4 months (Fig 9A), and while three of  
7 the OPC-N2 had a similar distribution to the GRIMM (OPC12, 13 and 14), OPC9 appeared to  
8 show evidence for instrument drift as the mode has shifted relative to the GRIMM. However,  
9 the increased frequency of higher mass concentrations not observed by the GRIMM but by all  
10 four OPC-N2 (Fig 9A) suggests that ambient RH is also a factor, as the average RH in January  
11 (91%) was higher than September (84%). Therefore, we calculated the correction for RH as  
12 described in the previous section (Eqn 6), as changes in aerosol composition would affect the  
13 particle hygroscopicity. In addition, the  $\kappa$  was only fitted for the data with RH < 95% since the  
14 hygroscopicity of aerosol is highly sensitive to any error in the RH measurement above this  
15 value. Application of the RH correction factor resulted in better agreement between each of the  
16 OPC-N2, with similar corrected distributions observed (Fig 9B). Furthermore, the corrected  
17 OPC-N2 concentrations also had better agreement with the GRIMM during January (Fig 9B)  
18 compared to uncorrected concentrations (Fig 9A), suggesting that changes in the particle water  
19 content were the cause. Thus, at least over a four month measurement period, there appears to  
20 be no evidence for instrument drift in the OPC-N2, once appropriate correction factors were  
21 applied.

### 22 **3.4 Discussion on the OPC-N2 interferences**

23 In the previous sections, the significant positive artefact observed by the OPC-N2 relative to  
24 the reference instruments were at times when the ambient RH was high, pointing to particle  
25 water content as the cause. This result is perhaps not surprising, as many studies in the literature  
26 have shown that particle water content can be a major reason for discrepancies between  
27 techniques that measure ambient particle mass (See e.g. (Charron et al., 2004)). The use of  $\kappa$ -  
28 Kohler theory to derive a correction factor based on ambient RH improved the agreement  
29 between the OPC-N2 and reference instruments; however a limitation of this approach is that  
30 the bulk aerosol hygroscopicity is related to particle composition, typically the inorganic  
31 fraction (e.g. (Gysel et al., 2007)). Variation in ambient particle composition could account for  
32 the large spread observed in the ratio of OPC-N2/TEOM at high RH (Fig 7), as an average  
33 hygroscopicity correction will overestimate when PM with higher hygroscopicity is measured

1 and vice versa. Furthermore, Eqn 6 may not be required for locations where the ambient RH is  
2 lower than 85%, as typically atmospheric particle growth due to water below this threshold is  
3 limited and a simple linear regression may be sufficient. Thus, in-situ and seasonally specific  
4 calibrations for the OPC-N2 are required to account for possible differences in ambient aerosol  
5 properties. However as  $\kappa$  values for continental regions tend to fall within a narrow range  
6 globally ( $0.3 \pm 0.1$ , (Andreae and Rosenfeld, 2008), with some systematic deviations for certain  
7 regions (Pringle et al., 2010), this average  $\kappa$  value could be used in lieu of calibration with  
8 reference instrument (e.g. a TEOM) to determine the correction factor (C) according to Eqn 7:  
9

$$10 \quad C = 1 + \frac{0.3/1.65}{-1 + \frac{1}{a_w}} \quad (7)$$

11  
12 However, it should be noted that while *in situ* calibration of an OPC-N2 with suitable reference  
13 instrumentation is preferable, for many locations around the world, and especially low and  
14 middle income countries (LMICs), this may not be possible and so using an appropriate  $\kappa$  value  
15 from the literature in Eqn 7 may be a reasonable approximation.  
16

#### 17 **4.0 Applicability of OPC-N2 for ambient monitoring**

18 The Alphasense OPC-N2 was evaluated for use in ambient monitoring of airborne particle  
19 mass concentration, with TEOM-FDMS and two commercial optical light scattering  
20 instruments; GRIMM PAS 1.108 and TSI 3330 employed as reference instruments.  
21 Comparison of the OPC-N2 to the reference optical instruments demonstrated reasonable  
22 agreement for the measured mass concentrations of  $PM_{10}$ ,  $PM_{2.5}$  and  $PM_{10}$  as evidenced by the  
23 stated accuracy and precision. However, the OPC-N2 demonstrated a significant large positive  
24 artefact in measured particle mass during times of high ambient RH, and a calibration factor  
25 was developed based on bulk particle aerosol hygroscopicity. Application of the RH correction  
26 factor, based upon  $\kappa$ -Kohler theory, resulted in notable improvement with the corrected OPC-  
27 N2 measurements within 33% of a TEOM-FDMS. While higher than the slope of  $1 \pm 0.1$   
28 allowed by the US EPA, it is comparable to the agreement of a GRIMM to the TEOM (20%).  
29 All low cost PM sensors will likely require calibration factors to obtain the dry particle weight  
30 unless they actively dry the PM containing air stream before it enters the device. The use of  
31 heated inlets could be used to reduce the RH in the air stream but would have consequences on  
32 the power requirements of the sensor, potentially making them less attractive for battery led

1 operation. For PM<sub>10</sub> mass concentrations, a CV of 22+13% between the 14 OPC-N2  
2 employed in this study was observed, with some of the variability likely due to use of  
3 separate but identical inlets, and therefore could be considered reasonable for a low-cost  
4 sensor but this level of precision needs to be considered when using multiple units. One  
5 out of four OPC-N2 tested for long-term monitoring appeared to show evidence for instrument  
6 drift relative to reference instruments.

7 Overall, the OPC-N2 have been shown to accurately measure ambient airborne particle mass  
8 concentration provided they are correctly calibrated and corrected for RH. The reasonable level  
9 of precision demonstrated between multiple OPC-N2 suggests that they would be suitable for  
10 applications where a number of instruments are required such as spatial mapping and personal  
11 exposure studies.

12 **Acknowledgements**

13 The authors wish to thank Peter Porter and Birmingham City Council for help in collocating  
14 the sensors next to the Tyburn Road AURN site. Funding is acknowledged from EPSRC  
15 (Global Challenges Research Fund IS2016). AL and MS acknowledge funding from the  
16 NERC National Capability programme ACREW and NE/N007115/1

17  
18



## 1 **References**

- 2 Andrae, M.O., Rosenfeld, D., 2008. Aerosol–cloud–precipitation interactions. Part 1. The  
3 nature and sources of cloud-active aerosols. *Earth-Science Reviews* 89, 13-41.
- 4 Borrego, C., Costa, A.M., Ginja, J., Amorim, M., Coutinho, M., Karatzas, K., Sioumis, T.,  
5 Katsifarakis, N., Konstantinidis, K., De Vito, S., Esposito, E., Smith, P., André, N., Gérard,  
6 P., Francis, L.A., Castell, N., Schneider, P., Viana, M., Minguillón, M.C., Reimringer, W.,  
7 Otjes, R.P., von Sicard, O., Pohle, R., Elen, B., Suriano, D., Pfister, V., Prato, M., Dipinto, S.,  
8 Penza, M., 2016. Assessment of air quality microsensors versus reference methods: The  
9 EuNetAir joint exercise. *Atmospheric Environment* 147, 246-263.
- 10 Castellini, S., Moroni, B., Cappelletti, D., 2014. PMetro: Measurement of urban aerosols on a  
11 mobile platform. *Measurement* 49, 99-106.
- 12 Charron, A., Harrison, R.M., Moorcroft, S., Booker, J., 2004. Quantitative interpretation of  
13 divergence between PM10 and PM2.5 mass measurement by TEOM and gravimetric  
14 (Partisol) instruments. *Atmospheric Environment* 38, 415-423.
- 15 de Nazelle, A., Bode, O., Orjuela, J.P., 2017. Comparison of air pollution exposures in active  
16 vs. passive travel modes in European cities: A quantitative review. *Environment International*  
17 99, 151-160.
- 18 Gao, M., Cao, J., Seto, E., 2015. A distributed network of low-cost continuous reading  
19 sensors to measure spatiotemporal variations of PM2.5 in Xi'an, China. *Environmental*  
20 *Pollution* 199, 56-65.
- 21 Grover, B.D., Eatough, N.L., Eatough, D.J., Chow, J.C., Watson, J.G., Ambs, J.L., Meyer,  
22 M.B., Hopke, P.K., Al-Horr, R., Later, D.W., Wilson, W.E., 2006. Measurement of Both  
23 Nonvolatile and Semi-Volatile Fractions of Fine Particulate Matter in Fresno, CA. *Aerosol*  
24 *Science and Technology* 40, 811-826.
- 25 Gysel, M., Crosier, J., Topping, D.O., Whitehead, J.D., Bower, K.N., Cubison, M.J.,  
26 Williams, P.I., Flynn, M.J., McFiggans, G.B., Coe, H., 2007. Closure study between chemical  
27 composition and hygroscopic growth of aerosol particles during TORCH2. *Atmos. Chem.*  
28 *Phys.* 7, 6131-6144.
- 29 Hagan, D., 2017. py-opc, <https://github.com/dhhagan/py-opc>.
- 30 Holstius, D.M., Pillarisetti, A., Smith, K.R., Seto, E., 2014. Field calibrations of a low-cost  
31 aerosol sensor at a regulatory monitoring site in California. *Atmos. Meas. Tech.* 7, 1121-  
32 1131.
- 33 Hu, D., Qiao, L., Chen, J., Ye, X., Yang, X., Cheng, T., Fang, W., 2010. Hygroscopicity of  
34 inorganic aerosols: size and relative humidity effects on the growth factor. *Aerosol and Air*  
35 *Quality Research* 10, 255-264.
- 36 Kumar, P., Morawska, L., Martani, C., Biskos, G., Neophytou, M., Di Sabatino, S., Bell, M.,  
37 Norford, L., Britter, R., 2015. The rise of low-cost sensing for managing air pollution in  
38 cities. *Environment International* 75, 199-205.
- 39 Lewis, A.C., Lee, J.D., Edwards, P.M., Shaw, M.D., Evans, M.J., Moller, S.J., Smith, K.R.,  
40 Buckley, J.W., Ellis, M., Gillot, S.R., White, A., 2016. Evaluating the performance of low  
41 cost chemical sensors for air pollution research. *Faraday Discussions* 189, 85-103.
- 42 Manikonda, A., Zíková, N., Hopke, P.K., Ferro, A.R., 2016. Laboratory assessment of low-  
43 cost PM monitors. *Journal of Aerosol Science* 102, 29-40.
- 44 Mead, M.I., Popoola, O.A.M., Stewart, G.B., Landshoff, P., Calleja, M., Hayes, M., Baldovi,  
45 J.J., McLeod, M.W., Hodgson, T.F., Dicks, J., Lewis, A., Cohen, J., Baron, R., Saffell, J.R.,  
46 Jones, R.L., 2013. The use of electrochemical sensors for monitoring urban air quality in low-  
47 cost, high-density networks. *Atmospheric Environment* 70, 186-203.

1 Mueller, M., Meyer, J., Hueglin, C., 2017. Design of an ozone and nitrogen dioxide sensor  
2 unit and its long-term operation within a sensor network in the city of Zurich. *Atmos. Meas.*  
3 *Tech. Discuss.* 2017, 1-29.

4 Petters, M., Kreidenweis, S., 2007. A single parameter representation of hygroscopic growth  
5 and cloud condensation nucleus activity. *Atmospheric Chemistry and Physics* 7, 1961-1971.

6 Pope, F.D., 2010. Pollen grains are efficient cloud condensation nuclei. *Environmental*  
7 *Research Letters* 5, 044015.

8 Pope, F.D., Dennis-Smith, B.J., Griffiths, P.T., Clegg, S.L., Cox, R.A., 2010. Studies of  
9 single aerosol particles containing malonic acid, glutaric acid, and their mixtures with sodium  
10 chloride. I. Hygroscopic growth. *The Journal of Physical Chemistry A* 114, 5335-5341.

11 Popoola, O.A.M., Stewart, G.B., Mead, M.I., Jones, R.L., 2016. Development of a baseline-  
12 temperature correction methodology for electrochemical sensors and its implications for  
13 long-term stability. *Atmospheric Environment* 147, 330-343.

14 Pöschl, U., 2005. Atmospheric aerosols: composition, transformation, climate and health  
15 effects. *Angewandte Chemie International Edition* 44, 7520-7540.

16 Pringle, K.J., Tost, H., Pozzer, A., Pöschl, U., Lelieveld, J., 2010. Global distribution of the  
17 effective aerosol hygroscopicity parameter for CCN activation. *Atmos. Chem. Phys.* 10,  
18 5241-5255.

19 Rai, A., Kumar, P., Pilla, F., Skouloudis, A., Di Sabatino, S., Ratti, C., Yasar, A., Rickerby,  
20 D., 2017. End-user Perspective of Low-cost Sensors for Outdoor Air Pollution Monitoring.  
21 *Science of The Total Environment*.

22 Smith, K.R., Edwards, P., Evans, M.J., Lee, J.D., Shaw, M.D., Squires, F.A., Lewis, A.,  
23 2017. Clustering approaches to improve the performance of low cost air pollution sensors.  
24 *Faraday Discussions*, 1-15.

25 Snyder, E.G., Watkins, T.H., Solomon, P.A., Thoma, E.D., Williams, R.W., Hagler, G.S.W.,  
26 Shelow, D., Hindin, D.A., Kilaru, V.J., Preuss, P.W., 2013. The Changing Paradigm of Air  
27 Pollution Monitoring. *Environmental Science & Technology* 47, 11369-11377.

28 Sousan, S., Koehler, K., Hallett, L., Peters, T.M., 2016. Evaluation of the Alphasense optical  
29 particle counter (OPC-N2) and the Grimm portable aerosol spectrometer (PAS-1.108).  
30 *Aerosol Science and Technology* 50, 1352-1365.

31 Steinle, S., Reis, S., Sabel, C.E., Semple, S., Twigg, M.M., Braban, C.F., Leeson, S.R., Heal,  
32 M.R., Harrison, D., Lin, C., Wu, H., 2015. Personal exposure monitoring of PM<sub>2.5</sub> in indoor  
33 and outdoor microenvironments. *Science of The Total Environment* 508, 383-394.

34 Viana, M., Rivas, I., Reche, C., Fonseca, A.S., Pérez, N., Querol, X., Alastuey, A., Álvarez-  
35 Pedrerol, M., Sunyer, J., 2015. Field comparison of portable and stationary instruments for  
36 outdoor urban air exposure assessments. *Atmospheric Environment* 123, 220-228.

37 Yin, J., Harrison, R.M., Chen, Q., Rutter, A., Schauer, J.J., 2010. Source apportionment of  
38 fine particles at urban background and rural sites in the UK atmosphere. *Atmospheric*  
39 *Environment* 44, 841-851.

40